

# Traces of co-evolution in high $z$ X-ray selected and submm-luminous QSOs.

A. Khan-Ali<sup>1</sup>, F.J. Carrera<sup>1</sup>, M.J. Page<sup>2</sup>, J.A. Stevens<sup>3</sup>, S. Mateos<sup>1</sup>, M. Symeonidis<sup>2,4</sup> and J.M. Cao Orjales<sup>3</sup>

<sup>1</sup> Instituto de Física de Cantabria (CSIC-UC), Santander 39005, Spain.

<sup>2</sup> Mullard Space Science Laboratory, University College London, RH5 6NT, UK.

<sup>3</sup> Centre for Astrophysics Research, University of Hertfordshire, AL10 9AB, UK.

<sup>4</sup> University of Sussex, Department of Physics and Astronomy, BN1 9QH, Sussex, UK.

## Abstract

We present a detailed study of a X-ray selected sample of 5 submillimeter bright QSOs at  $z \sim 2$ , where the highest rates of star formation (SF) and further growth of black holes (BH) occur. Therefore, this sample is a great laboratory to investigate the co-evolution of star formation and AGN. We present here the analysis of the spectral energy distributions (SED) of the 5 QSOs, including new data from Herschel PACS and SPIRE. Both AGN components (direct and reprocessed) and like Star Formation (SF) are needed to model its SED. From the SED and their UV-optical spectra we have estimated the mass of the black hole ( $M_{BH} = 10^9 - 10^{10} M_{SUN}$ ) and bolometric luminosities of AGN ( $L_{BOL} = (0.8 - 20) \times 10^{13} L_{SUN}$ ). These objects show very high luminosities in the far infrared range (at the H/ULIRG levels) and very high rates of SF ( $SFR = 400-1400 M_{SUN}/y$ ). Known their current SFR and their BH masses, we deduce that their host galaxies must be already very massive, or would not have time to get to the local relation between BH mass and bulge. Finally, we found evidence of a possible correlation between the column density of ionized gas detected in X-rays ( $NH_{ion}$ ) and SFR, which would provide a link between AGN and SF processes.

## 1 Introduction

In the last two decades, it has become clear that most local spheroidal galaxy components (elliptical galaxies and the bulges of spiral galaxies) contain a super massive black hole (SMBH) in their centres. The proportionality between black hole (BH) and spheroid mass suggests a direct link between the growth of the black hole as an Active Galactic Nucleus (AGN) and the stellar mass of the spheroid (e.g. [11], [9]). Identifying the main mechanisms for formation and evolution of galaxies, and their interrelation to that of the growth of their central black holes is a major issue in Astrophysics and Cosmology. In this work, we have studied a

sample of X-ray-obscured QSOs, described by [15] and [27], and studied by [26, 28], [16] and [4], at  $z \sim 1-3$  when most of the SF and BH growth are occurring in the Universe. These QSOs have strong submm emission, much higher than typically found in QSOs at similar redshifts and luminosities. [27] found detections at  $> 5\sigma$  significance at  $850\mu\text{m}$  (SCUBA). Here, we endeavour to get the physical properties of the central QSOs (luminosities, BH masses, Eddington ratios, etc.) and their host galaxies (SFR,  $M_{DUST}$ ,  $M_{GAS}$ , etc.) and their mutual relationships (or lack thereof). In addition, we will try to fathom their place in AGN-host galaxy co-evolution models.

## 2 Results

We have constructed the spectral energy distributions (SED) of all our objects, in  $\nu L_\nu$ . All objects clearly show at least two components: an UV-NIR contribution attributable to direct accretion disk emission (as expected from their type 1 nature), intrinsically absorbed in the cases of RX J0941 and RX J1218; and a reprocessed thermal component in the MIR region from warm optically thick dust further away from the nucleus (the torus). In all of them we also observe an additional FIR/submm component associated to cooler dust, heated by star formation (SF). We thus confirm the presence of strong FIR emission due to SF in these objects, at the ULIRG/HLIRG level (compared to e.g. Mrk 231).

Our next goal is to make fits to our data with different templates to extract quantitative information about our objects. We have selected the *Sherpa: CIAO's modeling & fitting package* [5] module for the Python platform to perform the fitting. SEDs were fitted in  $\nu L_\nu$  versus rest-frame  $\lambda$ . We use relatively simple empirical and theoretical templates, aiming at reproducing the general shape of the SEDs of our objects. We do not attempt to extract detailed physical information about our objects from those templates, since our data do not warrant such undertaking, and the underlying physics is likely to be more complex than that considered in the models. We have modelled the distinct constituents with three different components:

**An AGN accretion disk component:** This template models the direct emission from the accretion disk of the AGN (sub-parsec scales). We use the pure disk newAGN4 template from [23], affected by intrinsic extinction (see below). The only free parameter is the normalization of the template. We have normalized the template to its integral in the  $0.12-100\mu\text{m}$  range (standard limits used to estimate the accretion disk luminosity). From the fits we directly obtain the value of the disk luminosity in that range,  $L_{DISK}$ .

**A torus component:** This template models the re-emission from the warm and hot dust (on tens of parsecs scales, beyond the sublimation radius, see [2]) that is warmed by the accretion disk emission. We have used both an empirical template from [23] (dusttor, based on an average quasar spectrum) and three dusty clumpy torus models from [12] found by [20] to represent the average properties of type 1 QSOs (torus1, torus2 and torus3). Similarly, we have normalized them to their integral in the  $1-300\mu\text{m}$  range (again, standard limits used for the torus luminosity), so the only free parameter is  $L_{TORUS}$ .

**A SF component:** we have used a subset of the [24] spherical smooth models, found

Table 1: Average results and dispersions of fit parameters for each QSO, except for the X-ray AGN luminosity  $L_{X,AGN}$  which comes from [16].  $\chi^2$  represents the minimum value for each best-fit family and  $N$  represents the number of photometric points that we have for each object.

| Object   | $L_{X,AGN}$<br>( $10^{11} L_{\odot}$ ) | $N_H$<br>( $10^{20} \text{ cm}^{-2}$ ) | $L_{DISK}$<br>( $10^{11} L_{\odot}$ ) | $L_{TORUS}$<br>( $10^{11} L_{\odot}$ ) | $L_{FIR}$<br>( $10^{11} L_{\odot}$ ) | $L_{IR}$<br>( $10^{11} L_{\odot}$ ) | $\chi^2$ / N |
|----------|--|--|---------------------------------------|--|--------------------------------------|-------------------------------------|--------------|
| RX J0057 | 2.93                                   | $0.01 \pm 0.05$                        | $125 \pm 2$                           | $192 \pm 2$                            | $49 \pm 6$                           | $174 \pm 8$                         | 159 / 20     |
| RX J0941 | 0.93                                   | $0.77 \pm 0.11$                        | $100 \pm 3$                           | $148 \pm 9$                            | $78 \pm 6$                           | $179 \pm 13$                        | 347 / 23     |
| RX J1218 | 2.33                                   | $0.39 \pm 0.08$                        | $42 \pm 7$                            | $25 \pm 3$                             | $63 \pm 4$                           | $90 \pm 11$                         | 414 / 17     |
| RX J1249 | 3.69                                   | $0.14 \pm 0.03$                        | $1230 \pm 70$                         | $1156 \pm 8$                           | $70 \pm 13$                          | $782 \pm 19$                        | 3109 / 23    |
| RX J1633 | 5.85                                   | $0.003 \pm 0.002$                      | $64.9 \pm 0.6$                        | $74 \pm 5$                             | $22 \pm 2$                           | $90 \pm 5$                          | 29 / 17      |

by [29] to encompass the observed SEDs of star-forming galaxies at least up to  $z \sim 2$ . The full [24] models have five free parameters to obtain their 7000 templates. The subset of templates recommended by [29] (around 2000 templates) are divided into 11 sub-grids, depending on the maximum radius and different star populations. For each source, we found the best-fit template for each of these 11 sub-grids. We did not attempt to extract detailed physical information from the particular best-fit templates, since instead we were looking for physically-motivated templates that reproduced the spectral shape of the data. Therefore, the only parameter that we obtained from these fits, was the integrated FIR luminosity (40-500 $\mu\text{m}$ )  $L_{FIR}$ .

For each source (see below) we have chosen the family of models with the lowest  $\chi^2$ . Table 1 shows the average values of the luminosities and extinction values among each best-fit family for each source and the minimum value of  $\chi^2$  for each best-fit family. We have estimated the uncertainties in those values from the standard deviation. We believe that these values and their uncertainties are fair estimates of the luminosities of each component and of the effects of the photometric errors and our lack of an accurate physical model for what is really happening in each source.

### 3 Discussion

In this Section we will piece together the clues obtained above about the nature of our objects. We confirm the presence of strong FIR emission in these objects (well above that expected from plausible AGN emission models) which we attribute to SF at the ULIRG/HLIRG level with  $\text{SFR} \sim 1000 M_{\odot}/\text{y}$ . Their associated greybody temperature values are close to those of Submillimeter Galaxies (SMGs). They have dust masses around  $10^9 M_{\odot}$ .

The black holes powering our QSOs are very massive at their epoch,  $\sim 10^9 - 10^{10} M_{\odot}$  (measured from broad emission lines in their optical-UV spectra). We have calculated their mass-doubling timescale  $\tau$  and the time to reach the maximum BH mass observed locally ( $2 \times 10^{10} M_{\odot}$ ), concluding that they can not grow much more. A further hint in this direction comes from the high Eddington ratio of RX J1633 which, according to [7] should persist only

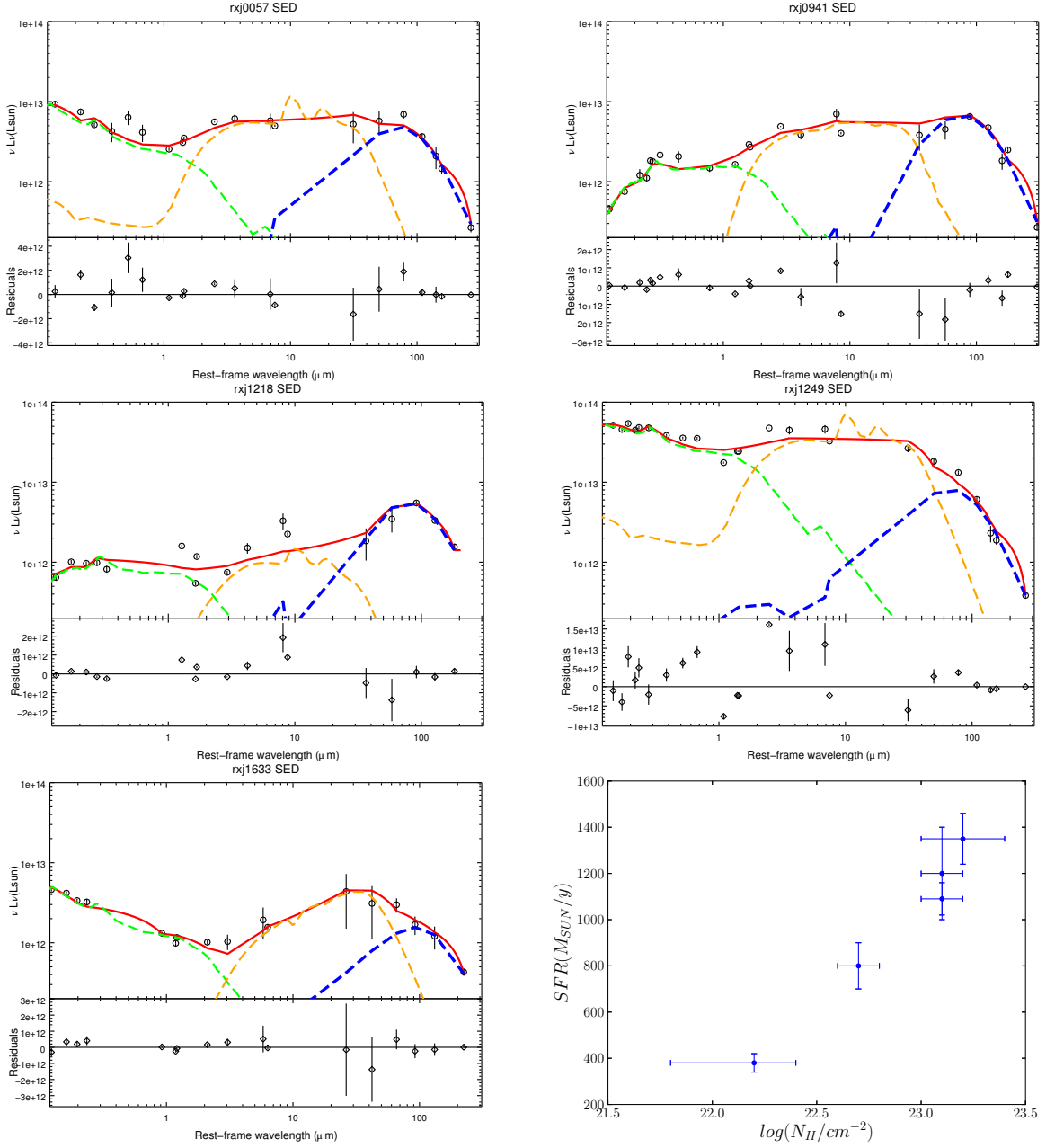


Figure 1: Each plot represents the combination of templates that best fits each SED. We show the total combined template (red solid line) and each individual component: obscured direct accretion disk (green dashed line), reprocessed in the torus (orange dashed line) and star formation (blue dashed line). For each source we also indicate below the torus component that provides the best-fit. **First row:** RX J0057: Torus1 (left column). RX J0941: Dusttor (right column). **Second row:** RX J1218: Torus2 (left column). RX J1249: Torus1 (right column). **Third row:** RX J1633: Torus3. (left column). Star formation rate versus  $N_{H_{\text{ion}}}$  for our sample. (right column)

Table 2: Additional physical quantities derived from the average values and dispersions of the best-fit parameters and Summary of timescales for QSOs and star formation, assuming constant mass accretion rates and SFR.  $\tau$  is the black hole mass-doubling timescale, and  $\tau_{SB}$  is the time needed to reach the corresponding maximum host galaxy mass.  $t$  is the “look-back time”.

| Object   | $L_{BOL}$<br>( $10^{11} L_{\odot}$ ) | CF                | $SFR$<br>( $M_{\odot} y^{-1}$ ) | $\log(M_{BH})$<br>( $\log(M_{\odot})$ ) | $\tau$<br>( $Gy$ )     | $\tau_{SB}$<br>( $Gy$ ) | $t$<br>( $Gy$ ) |
|----------|--------------------------------------|-------------------|---------------------------------|---|------------------------|-------------------------|-----------------|
| RX J0057 | $246.6 \pm 1.0$                      | $0.78 \pm 0.01$   | $800 \pm 100$                   | $9.94 \pm 0.36$                         | $0.5^{+0.3}_{-0.4}$    | $10.7 \pm 1.3$          | 10.6            |
| RX J0941 | $169.3 \pm 1.2$                      | $0.87 \pm 0.05$   | $1350 \pm 110$                  | $9.77 \pm 0.40$                         | $0.5^{+0.3}_{-0.4}$    | $6.32 \pm 0.5$          | 10.0            |
| RX J1218 | $78 \pm 4$                           | $0.32 \pm 0.04$   | $1090 \pm 70$                   | $9.28 \pm 0.45$                         | $0.4^{+0.2}_{-0.3}$    | $7.8 \pm 0.5$           | 9.9             |
| RX J1249 | $1890 \pm 30$                        | $0.613 \pm 0.012$ | $1200 \pm 200$                  | $9.99 \pm 0.45$                         | $0.08^{+0.06}_{-0.07}$ | $7.1 \pm 1.2$           | 10.6            |
| RX J1633 | $185.5 \pm 0.4$                      | $0.40 \pm 0.03$   | $380 \pm 40$                    | $8.73 \pm 0.36$                         | $0.04^{+0.02}_{-0.04}$ | $22 \pm 2$              | 11.3            |

for a very brief period of time. RX J1249 could become one of the most massive objects known. We do not know the masses of their host galaxies, but their black hole masses and their high SFR lead us to conclude that they are already very massive or they would not have enough time to reach the local bulge-to-black-hole-mass ratio. This is also in agreement with recent models of AGN-host galaxy co-evolution, e.g. the recent recently proposed by [10]. Our objects, with  $0.04 < L_{FIR}/L_{BOL} < 0.81$  would be in a stage when the FIR-luminous phase has ended (Figure 15 in [10]), in qualitative agreement with our conclusion that their host galaxies are already mostly formed.

Previous works have found some evidence of a correlation between the SF of the host and the AGN obscuration in the X-rays ([1], [3], [6], [21]). Later studies with deeper surveys both in the X-ray and infrared ranges have failed to reproduce these results (e.g [19], [22]). We have therefore looked for a correlation between  $N_{H_{ion}}$  (from [16]) and SFR in our sources (Fig. 1 fifth row right column), finding a tentative positive correlation between these parameters. This is interesting, since it would imply a coupling of the ionized gas absorbing the X-rays at the scale of the accretion disk or the BLR with the gas forming stars in the host galaxy bulge, about three orders of magnitude farther away. At face value, this would be compatible with a positive feedback scenario, [8] in which the ionized outflowing gas would trigger star formation in the interstellar medium of the host galaxy, with the highest column density gas corresponding to stronger feedback.

## Acknowledgments

A.K.A, F.J.C. and S.M. acknowledge financial support from the Spanish Ministerio de Economía y Competitividad. under project AYA2012-31447. SM acknowledges Financial support from the ARCHES project (7th Framework of the European Union, No. 313146).

## References

- [1] Alexander D. M., Bauer F. E., Chapman S. C., Smail I., Blain A. W., Brandt W. N., Ivison R. J., 2005, *ApJ*, 632, 736
- [2] Antonucci R., 1993, *ARA&A*, 31, 473
- [3] Bauer F. E., Alexander D. M., Brandt W. N., Hornschemeier A. E., Vignali C., Garmire G. P., Schneider D. P., 2002, *AJ*, 124, 2351
- [4] Carrera F. J., Page M. J., Stevens J. A., Ivison R. J., Dwelly T., Ebrero J., Falocco S., 2011, *MNRAS*, 413, 2791
- [5] Freeman P., Doe S., Siemiginowska A., 2001, *SPIE*, 4477, 76
- [6] Georgakakis A., Hopkins A. M., Afonso J., Sullivan M., Mobasher B., Cram L. E., 2004, *MNRAS*, 354, 127
- [7] Kelly B. C., Shen Y., 2013, *ApJ*, 764, 45
- [8] King A. L., et al., 2013, *ApJ*, 762, 103
- [9] Kormendy J., Ho L. C., 2013, *ARA&A*, 51, 511
- [10] Lapi A., Raimundo S., Aversa R., Cai Z.-Y., Negrello M., Celotti A., De Zotti G., Danese L., 2014, *ApJ*, 782, 69
- [11] Marconi A., Risaliti G., Gilli R., Hunt L. K., Maiolino R., Salvati M., 2004, *MNRAS*, 351, 169
- [12] Nenkova M., Sirocky M. M., Nikutta R., Ivezić Ž., Elitzur M., 2008, *ApJ*, 685, 160
- [13] Page M. J., Mittaz J. P. D., Carrera F. J., 2000, *MNRAS*, 318, 1073
- [14] Page M.J., Stevens J.A., Mittaz J.P.D., Carrera F.J., 2001, *Science*, 294, 2516
- [15] Page M. J., Stevens J. A., Ivison R. J., Carrera F. J., 2004, *ApJ*, 611, L85
- [16] Page M. J., Carrera F. J., Stevens J. A., Ebrero J., Blustin A. J., 2011, *MNRAS*, 416, 2792
- [17] Page M. J., et al., 2012, *Natur*, 485, 213
- [18] Richards G. T., et al., 2006, *ApJS*, 166, 470
- [19] Rosario D. J., et al., 2012, *A&A*, 545, A45
- [20] Roseboom I. G., Lawrence A., Elvis M., Petty S., Shen Y., Hao H., 2013, *MNRAS*, 429, 1494
- [21] Rovilos E., Georgakakis A., Georgantopoulos I., Afonso J., Koekemoer A. M., Mobasher B., Goudis C., 2007, *A&A*, 466, 119
- [22] Rovilos E., et al., 2012, *A&A*, 546, A58
- [23] Rowan-Robinson M.J., Babbedge T., Oliver S., Trichas M., et al., 2008, *MNRAS*, 368, 697
- [24] Siebenmorgen R., Krügel E., 2007, *A&A*, 461, 445
- [25] Stevens J. A., et al., 2003, *Natur*, 425, 264
- [26] Stevens J.A., Page M.J., Ivison R.J., Smail I., Carrera F. J., 2004, *ApJ*, 604, L17
- [27] Stevens J. A., Page M. J., Ivison R. J., Carrera F. J., Mittaz J. P. D., Smail I., McHardy I. M., 2005, *MNRAS*, 360, 610
- [28] Stevens J. A., Jarvis M. J., Coppin K. E. K., Page M. J., Greve T. R., Carrera F. J., Ivison R. J., 2010, *MNRAS*, 405, 2623
- [29] Symeonidis M., et al., 2013, *MNRAS*, 431, 2317